Geothermics 119 (2024) 102957

Contents lists available at ScienceDirect

Geothermics

journal homepage: www.elsevier.com/locate/geothermics

Using thermal response factors with time dependent thermal properties

Stephan Düber [a,b,*], Raul Fuentes [a], Guillermo A. Narsilio [b]

[a] Institute of Geomechanics and Underground Technology, RWTH Aachen University, Mies-van-der-Rohe-Str. 1 Aachen, 52074, Germany
[b] Department of Infrastructure Engineering, The University of Melbourne, Parkville, Australia

ARTICLE INFO

Keywords:
Thermal response factor
g-function
Thermal properties
Variable conductivity
Time dependent properties

ABSTRACT

This paper presents a simple and fast methodology to consider changing thermal properties in, for example, the design of shallow geothermal systems, by using thermal response factors. The simulation period is split into multiple sections according to the changes in thermal properties. By transforming the temperature response from one section to the next and subsequent superposition, any changes in the thermal conductivity properties of the media through which heat travels can be taken into account. The method is verified by numerical simulation and its efficiency is demonstrated in an application example. Results show that even though the computational effort increases exponentially with the variation of thermal parameters in time, the computational time is significantly shorter than comparable numerical simulations.

1. Introduction

Thermal response factors, also known as g-functions (Eskilson, 1987), are one of the main methods for designing shallow geothermal systems such as borehole heat exchangers, energy piles or horizontal geothermal collectors. The g-functions describe the dimensionless, time-dependent thermal resistance of the ground and allow the calculation of temperature changes due to heat conduction (Ingersoll et al., 1954):

$$\Delta T(t) = \frac{q}{2\pi\lambda} \cdot g(t). \tag{1}$$

Here λ is the thermal conductivity of the ground, q the thermal load, and g is the g-function of the heat exchanger, depending on its geometry and a dimensionless time. Starting from the infinite line source (Ingersoll et al., 1954), more and more analytical approaches have been developed in recent years to calculate the g-functions. For borehole heat exchangers and energy piles, the heat source radius (Man et al., 2010), finite length and surface effects (Zeng et al., 2002; Rivera et al., 2016), groundwater flow (Molina-Giraldo et al., 2011), layered soil types (Abdelaziz et al., 2014) and more realistic interaction between multiple boreholes (Cimmino and Bernier, 2014) can now be considered. Approaches for horizontal collectors can also take into account different geometries such as the slinky heat exchanger (Li et al., 2012) and the finite length of the pipes (Lamarche, 2019).

All of the approaches described above assume though that the thermal properties of the ground are constant over time. This assumption is generally justified in many cases, especially for deeper systems. However, it may be too simplistic for e.g., horizontal geothermal collectors or even energy piles, since the thermal properties may vary because of ground moisture content fluctuations due to seasonal changes or climate change (Leong et al., 1998). In these cases, time-demanding, more complex, numerical models are necessary to obtain an accurate response (Gan, 2019; Piechowski, 1999).

This paper fills this gap and presents a simple method to account for changing thermal properties using the thermal response factor method. The methodology is presented in detail in Section 2, followed by a verification and application example in Section 3, and finishing with conclusions in Section 4. A Python implementation of the proposed method is available online (Düber, 2023).

2. Methodology

The proposed method works with any type of g-function, but for illustration purposes, we use here a single buried pipe, for which the g-function is calculated using the horizontal finite line source (HFLS) as shown in Eq. (2). For more details on the derivation of Eq. (2), we refer the reader to the work of Lamarche (Lamarche, 2019).

$$g(t) = \int_{\frac{1}{\sqrt{4\alpha t}}}^{\infty} \frac{\left(e^{-r^2 s^2} - e^{-(r^2+4z^2)s^2}\right)}{Hs^2} \left[Hs\,\mathrm{erf}(Hs) - \frac{1}{\sqrt{\pi}}\left(1 - e^{-H^2 s^2}\right)\right] ds. \tag{2}$$

Here α denotes the thermal diffusivity of the ground, t the time, H the length of the line source, z its depth and r the horizontal distance where the temperature is evaluated. The temperature change $\Delta T(t)$ due

* Corresponding author at: Institute of Geomechanics and Underground Technology, RWTH Aachen University, Mies-van-der-Rohe-Str. 1 Aachen, 52074, Germany.
E-mail address: dueber@gut.rwth-aachen.de (S. Düber).

https://doi.org/10.1016/j.geothermics.2024.102957
Received 5 July 2023; Received in revised form 4 December 2023; Accepted 8 February 2024
Available online 17 February 2024

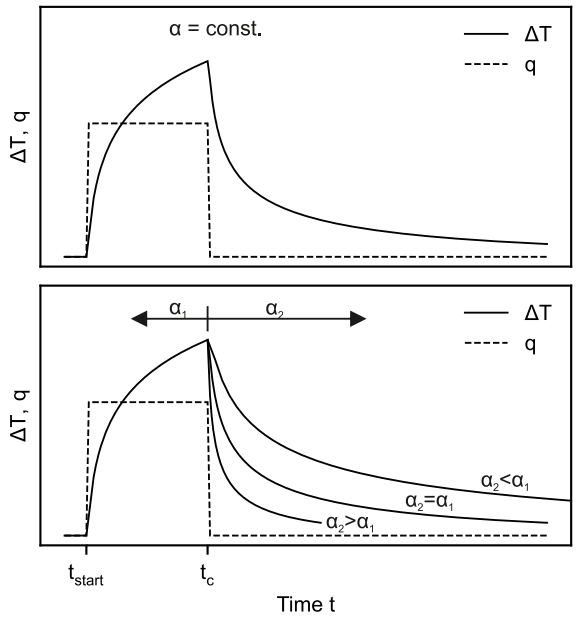

Fig. 1. Temperature change ΔT according to a constant load q between t_{start} and t_c for a typically assumed constant thermal parameter α of the heat transfer medium (top) and for the case when α changes for $t > t_c$ (bottom).

to a time-varying thermal load $q(t)$ is calculated using the g-function method and the superposition principle (Carslaw and Jaeger, 1959) as:

$$\Delta T(t_k) = \frac{1}{2\pi\lambda}\sum_{i=1}^{k}\Delta q(t_i)\cdot g(t_{k-i+1}) \tag{3}$$

where $\Delta q(t_i) = q(t_i) - q(t_{i-1})$ is the load increment, λ is the thermal conductivity of the ground and g the g-function according to Eq. (2).

Neither Eq. (3) nor the formulation of the g-function account for time dependent thermal properties of the ground. It means that, applying Eq. (3) for a constant load $q(t)$ for $t_{start} \le t \le t_c$ results in a $\Delta T(t)$ as shown in the top part of Fig. 1.

However, in reality, the thermal properties of the ground can change. Hence, if the thermal diffusivity α of the ground changes instantaneously at $t = t_c$, this change will only affect the temperature decay for $t > t_c$, as shown conceptually in the bottom part of Fig. 1.

As the temperatures for $t > t_c$ have been calculated using Eq. (3) for α_1, we suggest that there is no need to recalculate them for α_2. In fact, we propose that the change of α only causes a compression or stretching of the already calculated temperature change along the time axis. Hence, we can write for $t > t_c$:

$$\Delta T(\alpha_2, t) = \Delta T(\alpha_1, t\frac{\alpha_1}{\alpha_2} - t_c(\frac{\alpha_1}{\alpha_2} - 1)). \tag{4}$$

The factor $\frac{\alpha_1}{\alpha_2}$ accounts for a time stretching/compression of the temperature curve while $t_c(\frac{\alpha_1}{\alpha_2} - 1)$ corrects for the thereby introduced offset.

Fig. 2 shows conceptually what happens if the thermal property reduces from α_1 to α_2 at time $t = t_c$ (see solid line). The temperature will grow faster from $t = t_c$ until the time when $q = 0$, from which it will start a normal decay. The resulting curve is the superposition of the ΔT calculated using Eq. (3) for α_1, from $t = t_{start}$ to $t = t_c$, plus the same temperature response transformed for $t > t_c$, plus one calculated for α_2 from $t = t_c$ onward.

The method described can be used for any type of thermal load profile and for any variation in thermal conductivity or heat capacity. For an efficient implementation, we use the Fast Fourier Transform (FFT) as presented by Marcotte and Pasquier (2008), which replaces

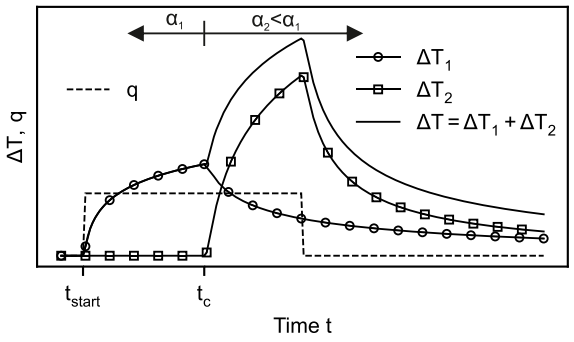

Fig. 2. Temperature change for a constant load with changing α at t_c as the sum of ΔT_1 and ΔT_2.

the summation over time in Eq. (3) with a single multiplication in the Fourier domain:

$$\Delta T = \mathcal{F}^{-1}\left(\mathcal{F}\left(\frac{\Delta q}{2\pi\lambda}\right)\cdot\mathcal{F}(g)\right) \tag{5}$$

where $\mathcal{F}$ is the direct and $\mathcal{F}^{-1}$ the inverse FFT. To ensure that Eq. (4) can be applied for any change in α, the simulation period must be extended. An increase in α results in a compression of the temperature response along the time axis, as can be seen in the bottom part of Fig. 1. To ensure that the transformed temperature response covers the entire simulation period, the maximum time t_{max} must be increased to t'_{max} as:

$$t'_{max} = \max\left(\{f(\alpha_j) : j = 1, \ldots, n\}\right) \tag{6}$$

with:

$$f(\alpha_j) = \frac{1}{\alpha_j}\left(\sum_{i=j}^{n-1}\alpha_i t_{c,i+1} - \sum_{i=j+1}^{n}\alpha_i t_{c,i} + \alpha_n t_{max}\right) \tag{7}$$

where n stands for the number of changes in α and $t_{c,i}$ for the times at which α changes. Finally, the implementation follows the flowchart presented in Fig. 3.

3. Verification and application

To verify the described approach, we compare it to a simulation using a 2D numerical finite volume model. The numerical model is spatially discretised with 600 × 600 cells each 10 × 10 mm in size. The temperatures on the cell walls are calculated using the central difference scheme while the explicit Euler scheme is used for the numerical integration. All parameters and boundary conditions are listed in Table 1. A large value was chosen for the length of the line source to minimise the influence of the finite length, which is not considered in the 2D numerical model. The radius in Table 1 denotes the horizontal distance from the line source where the temperature is evaluated. Using two thermal property changes over the calculation period, the results in Fig. 4 show perfect agreement between the numerical simulation and our approach. The numerical simulation took 181 s on a standard personal computer, while the computational time for the analytical approach was just 1.5 s.

To show how the method performs for a realistic scenario, we consider a single pipe of a horizontal geothermal collector buried 1.2 m below the surface exposed to the hourly load profile shown in Fig. 5. The load profile is derived from measurements of an operating geothermal system in Germany, all other parameters are given in Table 2.

For the ground it is assumed that the thermal properties change seasonally due to a change in the water content of the ground. The ground water content over central-western Europe can be approximated

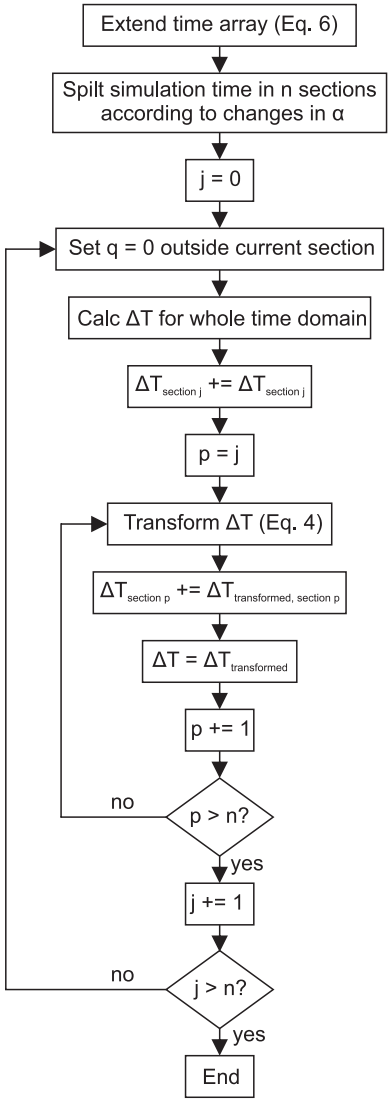

Fig. 3. Flowchart for the algorithm to account for arbitrary variations of α.

Table 1
Parameters used for verification simulation.

Parameter	Symbol	Value	Units
HFLS length	H	500	m
HFLS depth	z	0.85	m
Radius	r	0.2	m
Thermal load	q	30	$\mathrm{W\,m^{-1}}$
Thermal conductivity	λ	1.0 for $t < t_{c,1}$ 2.0 for $t_{c,1} \leq t < t_{c,2}$ 1.5 for $t \geq t_{c,2}$	$\mathrm{W\,m^{-1}\,K^{-1}}$
Volumetric heat capacity	ρc	1 000 000	$\mathrm{J\,m^{-3}\,K^{-1}}$
Simulation time	t_{max}	35	h
Time step	Δt	12.5	s
Time of change 1	$t_{c,1}$	41 675	s
Time of change 2	$t_{c,2}$	83 337.5	s

with a sinusoidal curve (Van der Linden et al., 2019). Here we assume for the thermal conductivity λ a value of $1.0\,\mathrm{W\,m^{-1}\,K^{-1}}$ for the dry and $2.2\,\mathrm{W\,m^{-1}\,K^{-1}}$ for the fully saturated case. The volumetric heat capacity ρc is considered to be $1.5\,\mathrm{MJ\,m^{-3}\,K^{-1}}$ for the dry and $2.2\,\mathrm{MJ\,m^{-3}\,K^{-1}}$ for the fully saturated case, resulting in the profile shown in Fig. 6. For the design or simulation of a real geothermal system, these values would ideally have to be measured. To understand

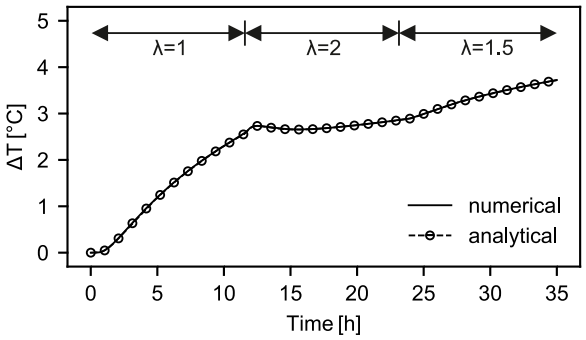

Fig. 4. Comparison of the proposed method with and numerical finite volume simulation.

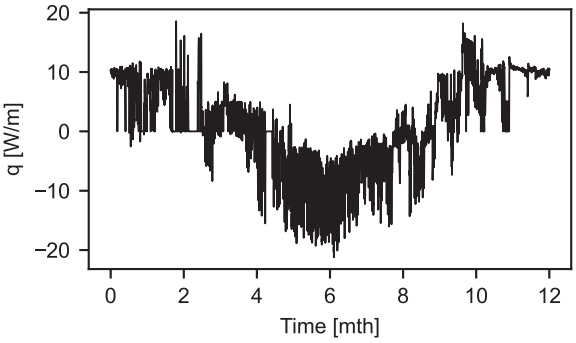

Fig. 5. Hourly load profile used for the application example.

Table 2
Parameters used for the application example.

Parameter	Symbol	Value	Units
HFLS length	H	20	m
HFLS depth	z	1.2	m
Radius	r	0.02	m
Thermal conductivity	λ	see Fig. 6	
Volumetric heat capacity	ρc	see Fig. 6	
Simulation time	t_{max}	8760	h
Time step	Δt	1200	s

the importance of ground property variations, we approximate the profile of the thermal properties with daily, monthly and three-monthly averages, resulting in 4, 12 and 365 values for α in the simulation. As we are only interested in the effect of the changes in the thermal properties, we neglect the course of the undisturbed ground temperature and restrict the analysis to the temperature change at the outside of the pipe introduced by the heat exchanger.

The top part of Fig. 7 shows the results for the simulation with averaged thermal properties ($\lambda = 1.6\,\mathrm{W\,m^{-1}\,K^{-1}}$, $\rho c = 1.85\,\mathrm{MJ\,m^{-3}\,K^{-1}}$) for the whole simulation period as reference. The lower parts show the temperature difference introduced by considering the different time resolution for changes in thermal properties. For the scenarios with 4 and 12 different values of α, the changes are clearly visible compared to the smooth curve for 365 values of α. The temperature difference introduced by the change in thermal properties is more than 2 °C, which is almost half of the temperature change caused by the heat exchanger when considering averaged properties (Fig. 7, top).

Finally, Table 3 shows the computational times of the proposed method compared to a 2D numerical model consisting of 1124 triangular elements simulated with the finite element software COMSOL Multiphysics™. The computational times of the proposed method increase exponentially with the number of changes in α. This is because

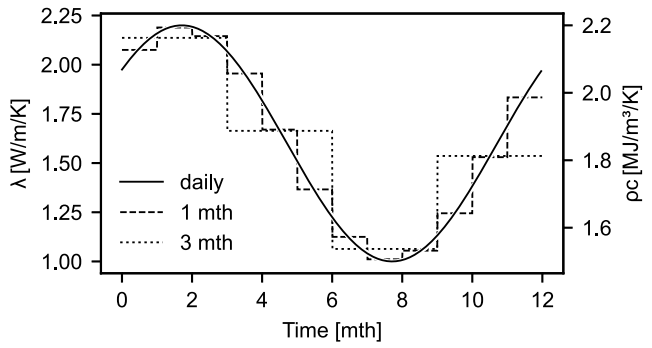

Fig. 6. Sinusoidal approximation of annual profile of the thermal properties. Daily, monthly and 3 monthly averaged values used as input for the simulation.

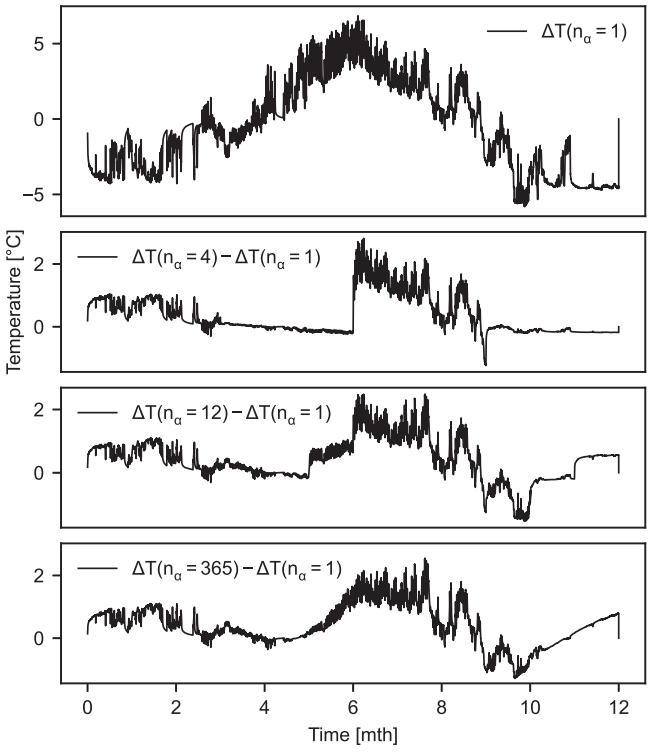

Fig. 7. Results of the application example with n_α values for α for the simulation period.

Table 3
Computational times [s] depending on the number of values for α.

n_α	Proposed method	2D numerical model
1	0.017	162
4	0.065	335
12	0.31	341
365	44.8	404

for each change, the response has to be transformed (Eq. (4)) for all subsequent values of α. However, even with daily updated values the total computation time is still only 44.8 s, clearly superior to the numerical simulation.

4. Conclusions

The use of thermal response factors is widespread in the simulation of shallow geothermal systems. While the thermal properties of the ground are rightly assumed to be constant for the simulation of borehole heat exchangers, typically 100 m or deeper, they can vary closer to the surface for a number of reasons over the life-time operation. This change, caused, for example, by varying groundwater levels or moisture content, can be relevant for systems such as horizontal geothermal collectors or shorter energy piles.

The proposed approach is a simple, yet efficient, method to account for changing thermal properties using the response factor method. One limitation is that the change in thermal properties is homogeneous, which is a simplification of the actual conditions. By dividing the simulation domain into several sections according to the changes in thermal properties and applying the superposition principle, arbitrary variations in thermal properties can be considered. The computational effort increases exponentially with the number of changes, but it is still considered superior to numerical simulations in many cases.

CRediT authorship contribution statement

Stephan Düber: Conceptualization, Formal analysis, Investigation, Methodology, Software, Validation, Visualization, Writing – original draft. **Raul Fuentes:** Supervision, Writing – review & editing. **Guillermo A. Narsilio:** Supervision, Writing – review & editing.

Declaration of competing interest

The authors declare that they have no known competing financial interests or personal relationships that could have appeared to influence the work reported in this paper.

Data availability

Data will be made available on request.

Acknowledgment

This work was supported by the RWTH Aachen - University of Melbourne Joint PhD Program.

References

Abdelaziz, S.L., Ozudogru, T.Y., Olgun, C.G., Martin, J.R., 2014. Multilayer finite line source model for vertical heat exchangers. Geothermics 51, 406–416. http://dx.doi.org/10.1016/j.geothermics.2014.03.004.

Carslaw, H.S., Jaeger, J.C., 1959. Conduction of Heat in Solids, third ed. Oxford University.

Cimmino, M., Bernier, M., 2014. A semi-analytical method to generate g-functions for geothermal bore fields. Int. J. Heat Mass Transfer 70, 641–650.

Düber, S., 2023. Varprop_gfunc. http://dx.doi.org/10.5281/zenodo.10209359, URL https://github.com/GUT-Aachen/varprop_gfunc.

Eskilson, P., 1987. Thermal analysis of heat extraction boreholes. (Ph. D. thesis). University of Lund, Lund, Sweden.

Gan, G.H., 2019. A numerical methodology for comprehensive assessment of the dynamic thermal performance of horizontal ground heat exchangers. Therm. Sci. Eng. Prog. 11, 365–379. http://dx.doi.org/10.1016/j.tsep.2019.04.013.

Ingersoll, L., Zobel, O., Ingersoll, A., 1954. Heat Conduction: With Engineering, Geological, and Other Applications. McGraw-Hill, New York.

Lamarche, L., 2019. Horizontal ground heat exchangers modelling. Appl. Therm. Eng. 155, 534–545. http://dx.doi.org/10.1016/j.applthermaleng.2019.04.006.

Leong, W., Tarnawski, V., Aittomäki, A., 1998. Effect of soil type and moisture content on ground heat pump performance: Effet du type et de l'humidité du sol sur la performance des pompes à chaleur à capteurs enterrés. Int. J. Refrig. 21 (8), 595–606.

Li, H., Nagano, K., Lai, Y.X., 2012. A new model and solutions for a spiral heat exchanger and its experimental validation. Int. J. Heat Mass Transfer 55 (15–16), 4404–4414. http://dx.doi.org/10.1016/j.ijheatmasstransfer.2012.03.084.

Man, Y., Yang, H., Diao, N., Liu, J., Fang, Z., 2010. A new model and analytical solutions for borehole and pile ground heat exchangers. Int. J. Heat Mass Transfer 53 (13–14), 2593–2601.

Marcotte, D., Pasquier, P., 2008. Fast fluid and ground temperature computation for geothermal ground-loop heat exchanger systems. Geothermics 37 (6), 651–665.

Molina-Giraldo, N., Blum, P., Zhu, K., Bayer, P., Fang, Z., 2011. A moving finite line source model to simulate borehole heat exchangers with groundwater advection. Int. J. Therm. Sci. 50 (12), 2506–2513.

Piechowski, M., 1999. Heat and mass transfer model of a ground heat exchanger: Theoretical development. Int. J. Energy Res. 23 (7), 571–588.

Rivera, J.A., Blum, P., Bayer, P., 2016. A finite line source model with Cauchy-type top boundary conditions for simulating near surface effects on borehole heat exchangers. Energy 98, 50–63. http://dx.doi.org/10.1016/j.energy.2015.12.129, Cited by: 44; All Open Access, Bronze Open Access.

Van der Linden, E., Haarsma, R., Schrier, G., 2019. Impact of climate model resolution on soil moisture projections in central-western europe. Hydrol. Earth Syst. Sci. 23, 191–206. http://dx.doi.org/10.5194/hess-23-191-2019.

Zeng, H.Y., Diao, N.R., Fang, Z.H., 2002. A finite line-source model for boreholes in geothermal heat exchangers. Heat Transfer—Asian Res. Co-sponsored Soc. Chem. Eng. Japan Heat Transfer Div ASME 31 (72), 558–567.